IEEE Access
Multidisciplinary ⋮ Rapid Review ⋮ Open Access Journal

Received 27 January 2023, accepted 15 February 2023, date of publication 22 February 2023, date of current version 8 March 2023.

Digital Object Identifier 10.1109/ACCESS.2023.3247507

RESEARCH ARTICLE

Quantum Geometric Transformation Based on QIRHSI Quantum Color images

XIANHUA SONG[1], GUANGLONG CHEN[2], AHMED A. ABD EL-LATIF[3,4], (Senior Member, IEEE), MUDASIR AHMAD WANI[3], AND BASSEM ABD-EL-ATTY[5]

[1]School of Science, Harbin University of Science and Technology, Harbin 150080, China
[2]School of Mathematics and Statistics, Lanzhou University, Lanzhou 730000, China
[3]EIAS Data Science Laboratory, College of Computer and Information Sciences, Prince Sultan University, Riyadh 11586, Saudi Arabia
[4]Department of Mathematics and Computer Science, Faculty of Science, Menoufia University, Shebeen El-Kom 6131567, Egypt
[5]Department of Computer Science, Faculty of Computers and Information, Luxor University, Luxor 85957, Egypt

Corresponding authors: Xianhua Song (songxianhua@hrbust.edu.cn) and Ahmed A. Abd El-Latif (ahmedabdellatif@ieee.org)

This work was supported by the EIAS Data Science Laboratory, College of Computer and Information Sciences, Prince Sultan University, Riyadh, Saudi Arabia.

ABSTRACT The negative effects caused by geometric distortion can be removed to the maximum extent possible through appropriate geometric transformations, allowing us to focus on the image content itself in subsequent processing and recognition. Therefore, geometric transformations are often used as a pre-processing step for other image processing applications. In this paper, quantum algorithms are designed to implement geometric transformations, including two-point swapping, circular translation, flipping transformations and right-angle rotation, across a quantum image representation QIRHSI (Quantum Image Representation based on HSI color space) which is built on HSI (Hue-Saturation-Intensity) color space. The above geometric transformations are realized by quantum circuits composed of elementary quantum gates. By analyzing the complexity of the fundamental quantum gates needed for the above geometric transformations, it is found that the global transformations (circular translation, flip transformation and right-angle rotation) are lower than the local transformation (two-point swapping). The proposed geometric transforms are used to facilitate the applications of quantum images with low complexity and high efficiency.

INDEX TERMS Quantum computation, quantum image representation, quantum geometric transformation, quantum circuit, complexity.

I. INTRODUCTION

The combination of quantum mechanics and computer science has given rise to a brand new discipline quantum computation [1]. As a new computing paradigm, it offers a possible solution to the failure of Moore's law [1]. Quantum computation has natural advantages [2], mainly in terms of quantum coherence, entanglement and superposition of quantum states, making quantum computation a greater advantage than traditional computation in terms of information storage and parallel computing. Therefore, quantum computation can solve those problems that are inefficiencies of traditional solutions. In 1994 Shor's polynomial-in-time algorithm for solving integer decomposition [3] and Grover's quadratic accelerated database search algorithm [4] are the most famous examples. These examples provide strong evidence for the superiority of quantum computers over classical computers.

The primary problem to be faced in the study of quantum image processing is the quantum image representation [5], [6], [7], [8], [9], [10], [11], [12], [13], [14], [15], [16], [17], [18], [19], [20], [21], [22], [23]. Common quantum image representation models (see Table 1) include Qubit Lattice [5], Real Ket [6], Entangled Image [7], Flexible Representation of Quantum Images (FRQI) [8], Multi-Channel Representation for Quantum Image (MCRQI) [9], Novel Enhanced Quantum Representation (NEQR) [10], Normal Arbitrary Quantum Superposition State (NAQSS) [11], Color Quantum Image

The associate editor coordinating the review of this manuscript and approving it for publication was Siddhartha Bhattacharyya.

TABLE 1. The different quantum image representation models.

QIR	Year	Inventor(s)	Required qubits	Color encoding	Complexity	Retrieval
QLM [5]	2003	Venegas-Andraca	2^{2n}	1 angle vectors (grayscale/RGB)	–	–
RKM [6]	2005	Latorre	–	quantum superposition	–	–
Entangled Image [7]	2010	Venegas-Andraca	–	binary geometrical shapes	–	–
FRQI [8]	2011	Le	$2n+1$	1 angle vectors (grayscale)	$O\left(2^{4n}\right)$	Probabilistic
MCRQI [9]	2011	Sun	$2n+3$	4 angle vectors (RGB)	$O\left(2^{4n+6}-3\cdot 2^{2n+3}\right)$	Probabilistic
NEQR [10]	2013	Zhang	$2n+q$	q qubits sequence (grayscale)	$O\left(qn\cdot 2^{2n}\right)$	Deterministic
NAQSS [11]	2014	Li	$2n+1$	1 angle vectors (grayscale/RGB)	$O\left(\log 2^{n}\cdot 2^{2n}\right)$	Probabilistic
CQIPT [12]	2014	Song	$2n+3$	4 angle vectors (RGB)	$O\left(2^{4n+5}-3\cdot 2^{2n+2}\right)$	Probabilistic
FQRCI [13]	2014	Yang	$2n+3$	3 angle vectors(RGB)	$O\left(3\cdot 2^{4n}\right)$	Probabilistic
SQR [14]	2014	Yuan	$2n+q+2$	1 angle vectors(infrared)	$\mathrm{O}\left(2^{2n}\right)$	Probabilistic
GQIR [15]	2015	Jiang	$h+w+q$	q qubits sequence (grayscale)	$\mathrm{O}\left(2^{4n+2}+qn2^{2n}\right)$	Deterministic
NCQI [16]	2016	Sang	$2n+3q$	$3q$ qubits sequence (RGB)	$\mathrm{O}\left(6qn\cdot 2^{2n}\right)$	Deterministic
BRQI [17]	2018	Li	$2n+4$ / $2n+6$	q / $3q$ qubits sequence (grayscale/RGB)	$\mathrm{O}\left(mn\cdot 2^{n}\right)$	Deterministic
OQIM [18]	2019	Xu	$2n+2$	1 angle vectors (grayscale)	$\mathrm{O}\left(2^{4n}\right)$	Probabilistic
QRCI [19]	2019	Wang	$2n+6$	q qubits sequence (RGB)	$\mathrm{O}\left(L\cdot 2^{2n}\right)$	Deterministic
FTQR [20]	2020	Grigoryan	$r+s$	Fourier transform representation (grayscale/ RGB)	$\mathrm{O}\left(r+s\right)$	Probabilistic
QHSL [21]	2021	Yan	$2n+q+1$	1 angle vectors and q qubits sequence (HSL)	$\mathrm{O}\left(24n+q-10\right)\cdot 2^{2n}$	Probabilistic/ Deterministic
QIRHSI [22]	2022	Chen	$2n+q+2$	2 angle vectors and q qubits sequence (HSI)	$O\left(2^{4n+2}+qn2^{2n}\right)$	Probabilistic/ Deterministic

based on Phase Transform (CQIPT) [12], Flexible Quantum Representation for Color Images (FQRCI) [13], Simple Quantum Representation (SQR) [14], Generalized Quantum Image Representation (GQIR) [15], Novel Quantum representation of Color digital Images (NCQI) [16], Bitplane Representation of Quantum Images (BRQI) [17], Order-encoded Quantum Image Model (OQIM) [18], Quantum Representation model of Color digital Images (QRCI) [19], Fourier Transform Qubit Representation (FTQR) [20], Quantum Hue, Saturation, and Lightness (QHSL) [21], Quantum Image Representation based on HSI color space (QIRHSI) [22], etc.

Ref. [15] tells us that there are two main current research directions in the field of quantum image processing: one deals with the representation of quantum images as shown in the previous paragraph, and the other with processing algorithms based on quantum images. And eight types of image processing algorithms are listed: simple geometric transformation [24], [25], [26], [27], image translation [28], [29], image scaling [15], [30], [31], [32], [33], color transformation [9], [10], [12], [16], [34], image scrambling [35], [36], [37], [38], image segmentation [7], [39], [40], [41], feature extraction [42], [43], quantum image watermarking [44], [45], [46], [47], [48], [49], [50], [51], [52], [53], image encryption [54], [55], [56], [57] and quantum image encryption [58], [59], [60], [61], [62], [63], [64], [65], [66], [67], [68], [69], [70].

Geometrical image modifications like coordinate transformations and local translation, inversion, reflection, stretching, and rotation require highly space-variant systems [71]. The polynomial interpolator structure can be used for high-quality geometric transformations of 2D and 3D images in traditional computer systems [72]. Many applications such as medical analysis, biomedical systems and image guidance require effective image geometrical transformation techniques [73].

Geometric transformation [24], [25], [26], [27], [28], [29] is one of the important elements of image processing and image analysis, but it is still in the infancy of quantum images. Le et al. proposed fast geometric transformations [24] based on FRQI representations such as two-point swapping, flips, coordinate swapping, orthogonal rotations and their variants of quantum images using elementary quantum gates, NOT, CNOT and Toffoli gates. The following year, Le et al. proposed three design strategies [25], including transformations of sub-blocks in quantum images, extending the separability of classical operations to quantum transformations, focusing on the smoothness of transformations that may not be

achieved using any of the earlier mentioned strategies. It is then used to construct new geometric transformations on FRQI quantum images form other transformations. In 2015, Wang, Jiang and Wang studied quantum image translations for the first time [28]. The entire and cyclic translation operations were proposed and quantum circuits for each of the two types of translation were given. In 2016, Fan et al. designed a new quantum algorithm to implement geometric transformations [26] based on Normal Arbitrary Superposition State (NASS) of n qubits, including two-point swapping, symmetric flip, local flip, orthogonal rotations and translations. In 2017, Zhou, Tan and Ian designed global translation and local translation based on quantum image FRQI [29]. The global translation is implemented using adder modulo N, and the local translation is implemented using Gray code, including single column translation, multi-column translation and translation of restricted areas. In the same year, Yan et al. proposed a new method for quantum image rotation based on the NEQR quantum image shear transformation [27]. The horizontal and vertical shear mapping required to compute the rotation was accomplished by designing three basic computational units, namely quantum self-adder, quantum control multiplier and quantum interpolation circuit.

Nowadays, there are two research directions based on geometric transformations of quantum image representations. One direction is to study more general geometric transformations based on quantum image representations, Zhang et al. proposed the affine transformation and the rotation transformation of arbitrary angle under the QUAntum Log-Polar Image (QUALPI) [74]. Based on the Flexible Log-Polar Image (FLPI) [75], an arbitrary rotational transformation was designed by Wang et al. The other direction is to study other operations on existing geometric transformations of quantum image representations, such as encryption, watermarking, etc. Zhou et al. in 2012 combined a variety of geometric transformations of quantum images to achieve encryption of quantum images, and also proposed two basic important contents: quantum grayscale image representation and quantum grayscale geometric transformation [76]. In 2014, Song et al. proposed a quantum image encryption scheme based on constrained geometric and color transformations [77]. In addition to this, Iliyasu et al. proposed a quantum computer image security based on restricted geometric transform with no key, blind watermarking and authentication strategy [45]. The above results show that there is a great need to explore the research in this direction.

Inspired by the quantum geometric transformation algorithms based on quantum image representations FRQI and NASS, we designed the geometric transformation algorithm for quantum image representation QIRHSI. Firstly, the quantum geometric transformation algorithm of FRQI is for grayscale images, the geometric transformation algorithm of NASS is for multi-dimensional images, and our designed quantum geometric transformation algorithm based on QIRHSI is constructed for color images. Secondly, it can better blend the quantum image representation QIRHSI-based geometric transformation algorithm into other quantum image algorithms, such as image encryption and image watermarking. Finally, the HSI model divides the image into color and grayscale information, making it more suitable for many grayscale processing techniques.

We use identify gates, NOT gates and multi-controlled not-gates as basic tools and aim to extend the use of quantum image representation models for different quantum image processing operations. The primary contribution of this paper is to give quantum geometric transformations based on the quantum image representation QIRHSI. In this paper, we analyze the complexity of quantum circuits using NOT gates and CNOT gates as the basic units.

(1) Based on the QIRHSI model, definition of the two-point swapping, circular translation, flipping transformation and right-angle rotation of the unitary operator are given, and the corresponding quantum circuits are given to analyze the complexity of different quantum geometric transformation operations in the form of theorems.

(2) The complexity of the quantum gates needed for different quantum geometry algorithms based on QIRHSI, FRQI and NAQSS models are compared, which corroborates from the side that the complexity of quantum geometry algorithms are closely related to the image size, but independent of the image color information.

The remainder of this paper is organized as follows. Section II introduces prior knowledge, with the basic quantum gates, the quantum color image representation QIRHSI, the plain adder and adder modulo N. Section III discusses in detail the geometric transformations based on QIRHSI images, including two-point swapping, circular translation, flipping transformations and right-angle rotation. The complexity comparison of the geometric transformations under different quantum image representation models are presented in Section IV. Experimental examples of the QIRHSI geometric transformation are given in Section V. The limitations of the geometric transformation algorithm are discussed in Section VI. Conclusions and future outlook are in Section VII.

II. PRIOR KNOWLEDGE

A. BASIC QUANTUM GATES

First, we give some basic quantum gates to describe the geometric transformation of the quantum image, as depicted in Figure 1. These circuits are executed from left to right, and each line in the circuit represents a wire. A quantum circuit is equivalent to the operation of a unitary matrix.

B. QIRHSI REPRESENTATION

We review how QIRHSI [22] represents a color image based on HSI color space. QIRHSI is an outstanding representation of quantum color images, which is derived from FRQI [8]

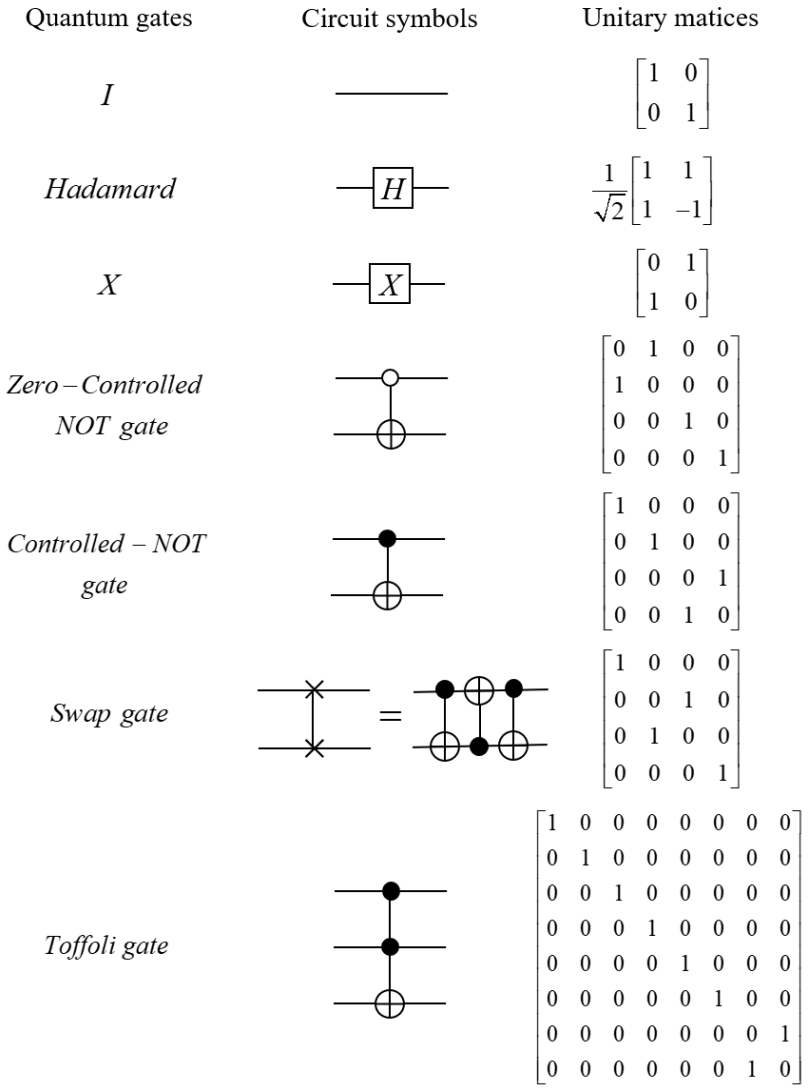

FIGURE 1. Some quantum basic gates, circuit symbols and corresponding unitary matrices.

and NEQR [10] model. According to the QIRHSI model, the quantum color image can be described as shown in Eq. (1).

$$\begin{aligned} |I(\theta)\rangle &= \frac{1}{2^n}\sum_{k=0}^{2^{2n}-1}|C_k\rangle\otimes|k\rangle \\ &= \frac{1}{2^n}\sum_{k=0}^{2^{2n}-1}|H_k\rangle|S_k\rangle|I_k\rangle\otimes|k\rangle \\ &= \frac{1}{2^n}\sum_{y=0}^{2^n-1}\sum_{x=0}^{2^n-1}\left|H_{yx}\right\rangle\left|S_{yx}\right\rangle\left|I_{yx}\right\rangle\otimes|yx\rangle \end{aligned} \tag{1}$$

wherein,

$$\begin{aligned} |H_k\rangle &= \cos\theta_{hk}|0\rangle + \sin\theta_{hk}|1\rangle \\ |S_k\rangle &= \cos\theta_{sk}|0\rangle + \sin\theta_{sk}|1\rangle \\ |I_k\rangle &= \left|C_k^0 C_k^1 \ldots C_k^{q-2} C_k^{q-1}\right\rangle \end{aligned}$$

$$\theta_{hk}, \theta_{sk} \in \left[0, 2^{-1}\pi\right], \quad C_k^m \in \{0, 1\}$$
$$m = 0, 1, \ldots, q-1$$
$$k = yx = 0, 1, \ldots, 2^{2n}-1$$

i.e. $|C_k\rangle$ and $|yx\rangle$ encode the color information and location information of the quantum color image, respectively. $|y\rangle = |y_{n-1}\ldots y_1 y_0\rangle$ signifies the first n-qubits along the vertical axis and $|x\rangle = |x_{n-1}\ldots x_1 x_0\rangle$ signifies the last n-qubits along the horizontal axis. A 4×4 color image and QIRHSI quantum state representation is provided in Figure 2.

C. PLAIN ADDER

To calculate the sum of the two numbers stored in the two quantum registers $|a\rangle$ and $|b\rangle$, it is necessary to rely on plain adder [78], [79].

Addition can be written in the following form.

$$|a,\ b,\ 0\rangle \rightarrow |a,\ b,\ a+b\rangle$$

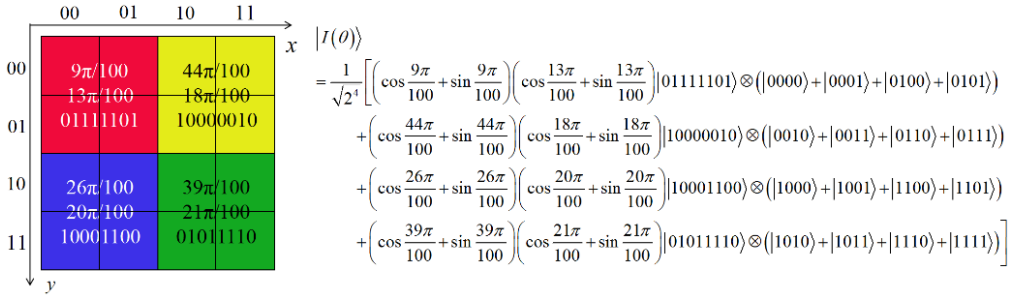

FIGURE 2. A 4 × 4 color image and QIRHSI quantum state representation.

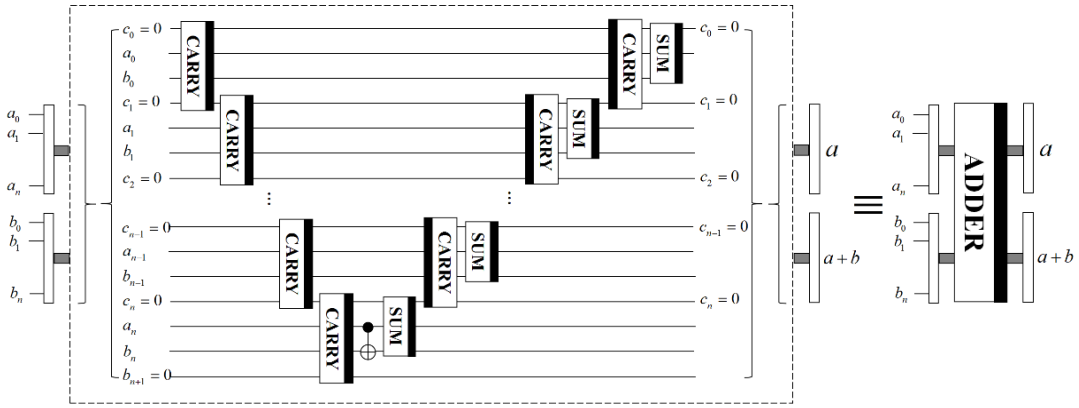

FIGURE 3. Plain adder network.

Rewrites the result of the calculation to one of the input registers, i.e.

$$|a,\ b\rangle \rightarrow |a,\ a+b\rangle \tag{2}$$

Figure 3 presents the network structure of the plain adder, where the sub-networks for the basic carry and sum operations are shown in Figure 4.

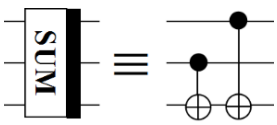

(a) The sum operation

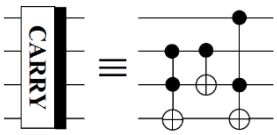

(b) The carry operation

FIGURE 4. Basic sum and carry operation.

D. ADDER MODULO N

The adder modulo N is a quantum network that is commonly used to calculate the modulo sum of two numbers [78], [79]. Its explicit form is illustrated in Eq. (3).

$$|a, b\rangle \rightarrow |a, (a+b)\ mod\ N\rangle \tag{3}$$

where $a, b \in [0, N)$. The quantum network structure of the adder modulo N is provided in Figure 5.

III. GEOMETRIC TRANSFORMATION OF QIRHSI IMAGE

Geometric transformations of the quantum grayscale image FRQI (two-point swapping, flipping, coordinate swapping and orthogonal rotation) [24] and the quantum color image NASS (two-point swapping, symmetric flip, local flip, orthogonal rotation and translation) [26] have been investigated so far. Based on these results, we have researched the geometric transformations of the quantum color image of QIRHSI [22], including two-point swapping, circular translation, flip transformation and right-angle rotation. Therefore, the general geometric transformation based on the quantum color image QIRHSI is defined as

$$G_T\left(|I\left(\theta\right)\rangle\right) = \frac{1}{2^n}\sum_{k=0}^{2^{2n}-1}|H_k\rangle|S_k\rangle|I_k\rangle \otimes G\left(|k\rangle\right) \tag{4}$$

where $|I\left(\theta\right)\rangle$ represents a QIRHSI quantum color image as shown in Eq. (1). The operator G_T for general geometric transformations can also be written as

$$G_T = I^{\otimes 2} \otimes I^{\otimes q} \otimes G \tag{5}$$

The quantum circuits of the general geometric transformation operator G_T based on the quantum color image QIRHSI are given in Figure 6.

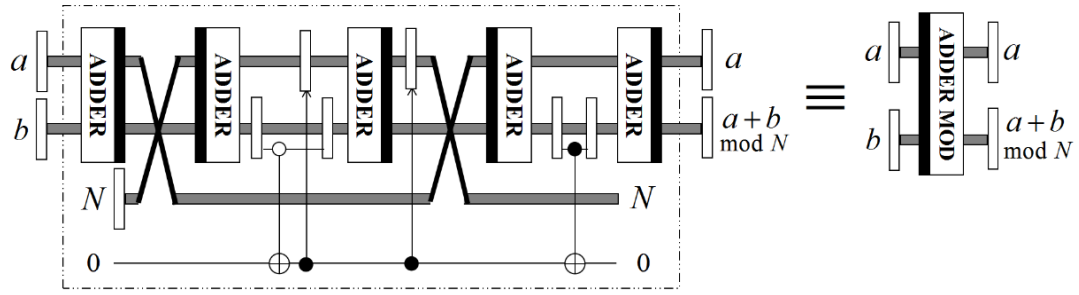

FIGURE 5. Adder modulo *N*.

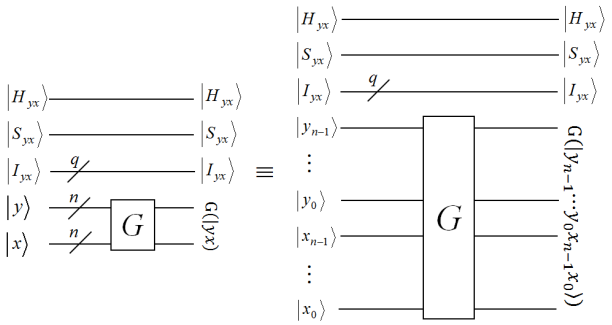

FIGURE 6. The universal circuit of quantum geometric transformations on QIRHSI images.

A. TWO-POINT SWAP

Definition 1: The two-point swap operator G_P based on QIRHSI color images is defined as

$$\begin{aligned} &G_P\left(|I(\theta)\rangle\right) \\ &= \frac{1}{2^n}\sum_{k=0}^{2^{2n}-1}|H_k\rangle|S_k\rangle|I_k\rangle\otimes P(|k\rangle) \\ &= \frac{1}{2^n}\left\{\begin{array}{l}|H_j\rangle|S_j\rangle|I_j\rangle\otimes|i\rangle+|H_i\rangle|S_i\rangle|I_i\rangle\otimes|j\rangle \\ +\sum_{k=0,k\neq i,j}^{2^{2n}-1}|H_k\rangle|S_k\rangle|I_k\rangle\otimes|k\rangle\end{array}\right\} \end{aligned} \tag{6}$$

where $|I(\theta)\rangle$ represents a QIRHSI color image, given in Eq. (1). The two-point swapping operator G_P can also be expressed as

$$\begin{aligned} G_P &= I^{\otimes 2}\otimes I^{\otimes q}\otimes P \\ &= I^{\otimes 2}\otimes I^{\otimes q}\otimes\left\{|i\rangle\langle j|+|j\rangle\langle i|+\sum_{k=0,k\neq i,j}^{2^{2n}-1}|k\rangle\langle k|\right\} \end{aligned} \tag{7}$$

From Eq. (7), we know that $P(|k\rangle)=|k\rangle$, $k\neq i,j$ and $P(|i\rangle)=|j\rangle$, $P(|j\rangle)=|i\rangle$.

In order to design quantum circuits based on the quantum image QIRHSI for the two-point swapping operator G_P, we need to use Gray code [1], [26]. Given two different binary numbers $i=i_{2n-1}\ldots i_1 i_0$ and $j=j_{2n-1}\ldots j_1 j_0$, the set of Gray codes connected to i and j is a set of binary numbers that starts with i and ends with j, such that the adjacent numbers differ by exactly one bit. For instance, for $2n$-bit binary numbers $i=0$ and $j=2^{2n}-1$, the binary expansion is shown in Eq. (8)

$$i=\underbrace{0\ldots0\ldots0}_{2n},\quad j=\underbrace{1\ldots1\ldots1}_{2n} \tag{8}$$

that there exists the following set of Gray codes presented in Eq. (9):

$$\begin{array}{cccccccccc} 0 & 0 & \ldots & 0 & 0 & 0 & \ldots & 0 & 0 \\ 0 & 0 & \ldots & 0 & 0 & 0 & \ldots & 0 & 1 \\ \vdots & \vdots & & \vdots & \vdots & \vdots & & \vdots & \vdots \\ 0 & 0 & \ldots & 0 & 1 & 1 & \ldots & 1 & 1 \\ \vdots & \vdots & & \vdots & \vdots & \vdots & & \vdots & \vdots \\ 0 & 1 & \ldots & 1 & 1 & 1 & \ldots & 1 & 1 \\ 1 & 1 & \ldots & 1 & 1 & 1 & \ldots & 1 & 1 \end{array} \tag{9}$$

Let g_1 to g_m be the elements of the Gray code that connects i and j, and $g_1=i$ to $g_m=j$. It is always to be found the Gray code that satisfies the condition $m\leq 2n+1$, as i and j have at most $2n$ positions of inconsistency [1].

Here is an example of a two-point swapping circuit implementation of a quantum color image QIRHSI with total 2^{2n} pixels as shown in Eq. (1). Suppose that the coordinates of the two pixels to be swapped in the QIRHSI image are $|i\rangle=|0\rangle$ and $|j\rangle=\left|2^{2n}-1\right\rangle$, and that the binary expansion of i and j is shown in Eq. (8). The Gray code connecting i and j is shown in Eq. (9). $|g_1\rangle=|i\rangle=|0\rangle$ to $|g_{2n+1}\rangle=|j\rangle=\left|2^{2n}-1\right\rangle$ are the elements of the Gray code. We just need to implement state transformations through a series of quantum gates

$$|g_1\rangle\rightarrow|g_2\rangle\rightarrow\ldots\rightarrow|g_{2n}\rangle \tag{10}$$

and then conduct multi-controlled NOT-gate operations with the target qubit at a different bit from $|g_{2n}\rangle$ and $|g_{2n+1}\rangle$, and then reduce the first stage of the operation and implement the transformation

$$|g_{2n}\rangle\rightarrow|g_{2n-1}\rangle\rightarrow\ldots\rightarrow|g_1\rangle \tag{11}$$

Finally, the swap of pixels $|i\rangle=|0\rangle$ and $|j\rangle=\left|2^{2n}-1\right\rangle$ of the quantum color image QIRHSI is realized. The quantum circuit for the QIRHSI color image implementing the two-point swap of pixels of $|i\rangle=|0\rangle$ and $|j\rangle=\left|2^{2n}-1\right\rangle$ is given in Figure 7.

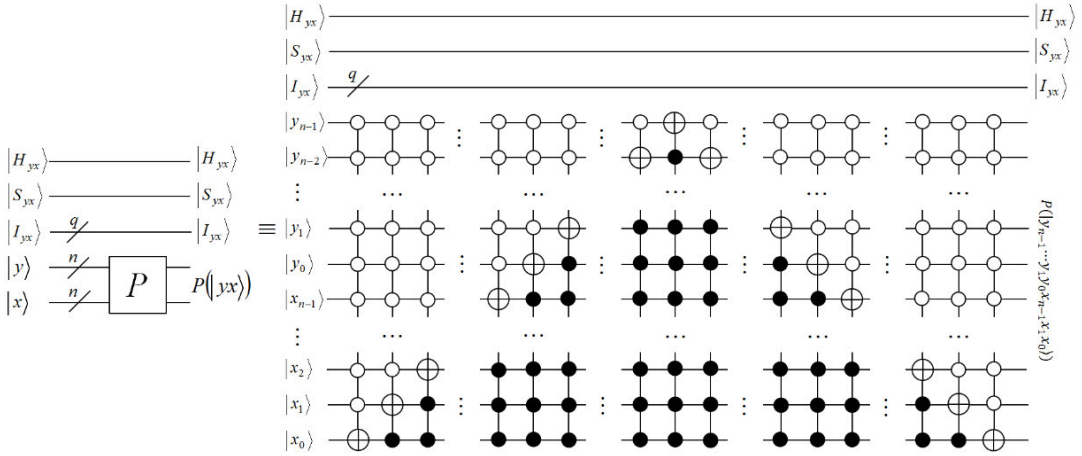

FIGURE 7. The quantum circuit of QIRHSI color images implementing the two-point swap of pixels $|i\rangle = |0\rangle$ and $|j\rangle = \left|2^{2n} - 1\right\rangle$.

Because more than one Gray code connecting i and j always exists, there is no unique that implements the swap between the two pixels of $|i\rangle$ and $|j\rangle$ [1]. For example, for $i = 0010$ and $j = 1111$, two Gray codes are shown in Eqs. (12) and (13).

$$\begin{matrix} 0 & 0 & 1 & 0 \\ 0 & 0 & 1 & 1 \\ 0 & 1 & 1 & 1 \\ 1 & 1 & 1 & 1 \end{matrix} \tag{12}$$

and

$$\begin{matrix} 0 & 0 & 1 & 0 \\ 1 & 0 & 1 & 0 \\ 1 & 1 & 1 & 0 \\ 1 & 1 & 1 & 1 \end{matrix} \tag{13}$$

Theorem 1: The complexity of the quantum gate required to implement the two-point swap operator G_P on the quantum image QIRHSI using Gray codes is $O\left(n^2\right)$.

Proof of Theorem 1: Let the pixel positions to be swapped in the quantum image QIRHSI by the two-point swapping operator G_P are $|i\rangle$ and $|j\rangle$, and the elements of a set of Gray codes connecting $2n$ bits of binary numbers i and j to $g_1,\ g_2,\ \ldots,\ g_{m-1},\ g_m$, where $g_1 = 0$, $g_m = 2^{2n} - 1$. The state transformations are implemented step by step using simply a series of quantum gates

$$|g_1\rangle \rightarrow |g_2\rangle \rightarrow \ldots \rightarrow |g_{m-1}\rangle$$

then multi-controlled NOT gate operations are conducted, followed by transformations

$$|g_1\rangle \rightarrow |g_2\rangle \rightarrow \ldots \rightarrow |g_{m-1}\rangle$$

the final result is the two-point swap operator G_P implemented in quantum circuits, with the required quantum gate complexity of $O\left(n^2\right)$ [1], [80]. In the following we will start to analyze the complexity of the quantum circuit in detail.

The first step is to swap the states of $|g_1\rangle$ and $|g_2\rangle$. Let $|g_1\rangle$ and $|g_2\rangle$ have different values for the lth bit, then we can complete the swap by flipping one of the controlled bits of the lth qubit, the condition to be satisfied is that the both $|g_1\rangle$ and $|g_2\rangle$ have the same qubit for the rest of the bits. Next, use a controlled operation to swap $|g_2\rangle$ and $|g_3\rangle$, and so on, until $|g_{m-2}\rangle$ and $|g_{m-1}\rangle$ have been swapped. The above $m-2$ operations complete the operations in Eq. (14)

$$\begin{aligned} |g_1\rangle &\rightarrow |g_{m-1}\rangle \\ |g_2\rangle &\rightarrow |g_1\rangle \\ |g_3\rangle &\rightarrow |g_2\rangle \\ &\ldots \\ |g_{m-1}\rangle &\rightarrow |g_{m-2}\rangle \end{aligned} \tag{14}$$

It should be noted that all other states of the computational basis remain unchanged during the sequence of operations. In the second step, let the w th bits of $|g_{m-1}\rangle$ and $|g_m\rangle$ are different, and under the condition that the other bits of $|g_{m-1}\rangle$ and $|g_m\rangle$ are the same, conduct a multi-control NOT gate operation targeting the wth qubit. Finally, the reductive swap operation is used to complete the multi-control NOT gate operation: $|g_{m-1}\rangle$ and $|g_{m-2}\rangle$ are swapped, followed by $|g_{m-2}\rangle$ and $|g_{m-3}\rangle$, and so on, until $|g_2\rangle$ and $|g_1\rangle$ are swapped.

Since i and j differ in at most $2n$ positions, it can always find a Gray code that satisfies $m \leq 2n + 1$ [1]. To implement the two-stage unitary operation up to $2\,(2n-1)$ controlled not-gate operations are required to swap $|g_1\rangle$ to $|g_{m-1}\rangle$ and back again. And each such controlled operation can be implemented using $O\,(n)$ NOT gates and multi control operation NOT gates. The achievement of a multi-control NOT gate operation with the wth qubit as the target also requires $O\,(n)$ elementary quantum gates. Thus, the implementation of $|g_1\rangle$ to $|g_{m-1}\rangle$ requires the quantum elementary gate of $O\left(n^2\right)$. Therefore, the complexity of the elementary quantum

gate required for the quantum circuit implementation of the two-point swap operator G_P on QIRHSI is $O\left(n^2\right)$.

B. CIRCULAR TRANSLATIONS

The circular translation of the QIRHSI image along the coordinate axis is described in Definition 2. Figure 8 gives an example of a circular translation of the image along the coordinate axis.

(a) Original Tree image (b) Circular translation along the y-axis (c) Circular translation along the x-axis

FIGURE 8. The image Tree was cyclically translated along the coordinate axis.

Definition 2: The operators T_{y+l} and T_{x+l} based on QIRHSI color image translated by l pixels along the y and x axis respectively are defined as

$$T_{y+l}\left(|I\left(\theta\right)\rangle\right) = \frac{1}{2^n}\sum_{y=0}^{2^n-1}\sum_{x=0}^{2^n-1}\left|H_{yx}\right\rangle\left|S_{yx}\right\rangle\left|I_{yx}\right\rangle\otimes\left|(y+l)\ mod\ 2^n, x\right\rangle \quad (15)$$

$$T_{x+l}\left(|I\left(\theta\right)\rangle\right) = \frac{1}{2^n}\sum_{y=0}^{2^n-1}\sum_{x=0}^{2^n-1}\left|H_{yx}\right\rangle\left|S_{yx}\right\rangle\left|I_{yx}\right\rangle\otimes\left|y, (x+l)\ mod\ 2^n\right\rangle \quad (16)$$

whereby $|I\left(\theta\right)\rangle$ represents a QIRHSI color image, see Eq. (1). $l = l_{n-1}\ldots l_1 l_0$ and $l \in (0, 2^n-1]$, so l_i $(i = 0, 1, \ldots, n-1)$ is not all zero. The translation operators T_{y+l} and T_{x+l} can be expressed respectively as

$$\begin{aligned} T_{y+l} &= I^{\otimes 2}\otimes I^{\otimes q}\otimes\sum_{j=0}^{2^n-1}\left|(j+l)\ \mathrm{mod}\ \ 2^n\right\rangle\langle j|\otimes I^{\otimes n} \\ &= I^{\otimes 2}\otimes I^{\otimes q} \\ &\quad\otimes\left\{\begin{array}{l}|(0+l)\ \mathrm{mod}\ \ 2^n\rangle\langle 0|+\ldots \\ +|(2^n-1+l)\ \mathrm{mod}\ \ 2^n\rangle\langle 2^n-1|\end{array}\right\}\otimes I^{\otimes n} \end{aligned} \quad (17)$$

$$\begin{aligned} T_{x+l} &= I^{\otimes 2}\otimes I^{\otimes q}\otimes I^{\otimes n}\otimes\sum_{j=0}^{2^n-1}\left|(j+l)\ \mathrm{mod}\ \ 2^n\right\rangle\langle j| \\ &= I^{\otimes 2}\otimes I^{\otimes q}\otimes I^{\otimes n} \\ &\quad\otimes\left\{\begin{array}{l}|(0+l)\ \mathrm{mod}\ \ 2^n\rangle\langle 0|+\ldots \\ +|(2^n-1+l)\ \mathrm{mod}\ \ 2^n\rangle\langle 2^n-1|\end{array}\right\} \end{aligned} \quad (18)$$

The quantum circuits of the circular translation operators T_{y+l} and T_{x+l} are given in Figures 9 and 10.

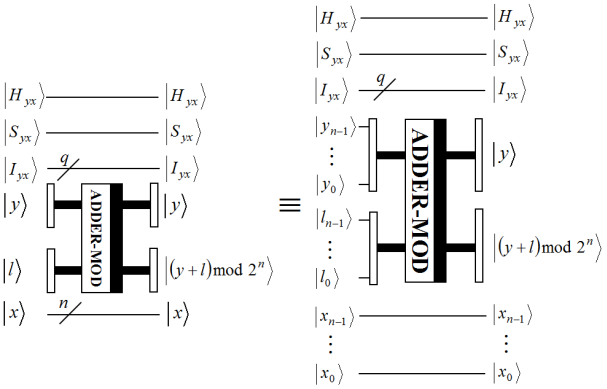

FIGURE 9. Quantum circuit of the QIRHSI image translated by *l* pixels along the *y* axis.

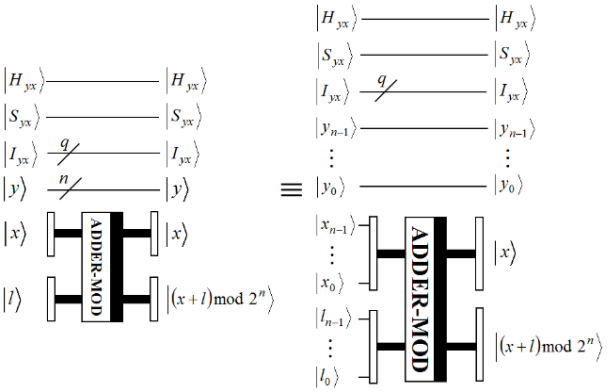

FIGURE 10. Quantum circuit of the QIRHSI image translated by *l* pixels along the *x* axis.

Theorem 2: The complexity of the quantum gates needed for the circular translation operators T_{y+l} and T_{x+l} on the quantum image QIRHSI is $O\left(n\right)$.

Proof of Theorem 2: In ordered to calculate the number of quantum gates required for the circular translation operators T_{y+l} and T_{x+l}, it is only needed to calculate the number of quantum elementary gates required for the module 2^n adder.

As one Toffoli gate is equivalent to six CNOT gates [78]. In the basic carry and sum operation (see Figure 4), the number of CNOT gates taken is 13 and 2 respectively. And the plain adder (see Figure 3) contains $2n-1$ carries, n sums and 1 CNOT gate, so the number of CNOT gates required for the plain adder is $28n-12$. The linear relationship with the input n of the quantum circuit.

The module 2^n adder (see Figure 5) contains 5 plain adders, 2 NOT gates and up to $2n+4$ CNOT gates. Thus, the module 2^n adder needs 2 NOT gates and up to $142n-56$ CNOT gates, i.e. the complexity of the quantum gates required for the module 2^n adder is $O\left(n\right)$. That is, the complexity of the quantum gates required for the circular translation operators T_{y+l} and T_{x+l} is $O\left(n\right)$.

C. FLIP TRANSFORMATIONS

The flip transformation of the QIRHSI image along the coordinate axis is shown in Definition 3. Figure 11 gives

an example of the image flipping transformation along the coordinate axis.

(a) Original Tree image (b) Flip it along the y-axis (c) Flip it along the x-axis

FIGURE 11. The image Tree was flipped along the coordinate axis.

Definition 3: The QIRHSI color image based flip transformation operators F_y and F_x along the y and x axis respectively are defined as

$$\begin{aligned} &F_y\left(|I\left(\theta\right)\rangle\right) \\ &= \frac{1}{2^n}\sum_{y=0}^{2^n-1}\sum_{x=0}^{2^n-1}\left|H_{yx}\right\rangle\left|S_{yx}\right\rangle\left|I_{yx}\right\rangle\otimes\left|y\bar{x}\right\rangle \\ &= \frac{1}{2^n}\sum_{y=0}^{2^n-1}\sum_{x=0}^{2^n-1}\left|H_{yx}\right\rangle\left|S_{yx}\right\rangle\left|I_{yx}\right\rangle\otimes\left|y,2^n-1-x\right\rangle \qquad (19) \\ &F_x\left(|I\left(\theta\right)\rangle\right) \\ &= \frac{1}{2^n}\sum_{y=0}^{2^n-1}\sum_{x=0}^{2^n-1}\left|H_{yx}\right\rangle\left|S_{yx}\right\rangle\left|I_{yx}\right\rangle\otimes\left|\bar{y}x\right\rangle \\ &= \frac{1}{2^n}\sum_{y=0}^{2^n-1}\sum_{x=0}^{2^n-1}\left|H_{yx}\right\rangle\left|S_{yx}\right\rangle\left|I_{yx}\right\rangle\otimes\left|2^n-1-y,x\right\rangle \qquad (20) \end{aligned}$$

where $|I\left(\theta\right)\rangle$ represents a QIRHSI color image, see Eq. (1). And

$$\begin{aligned} |y\rangle &= |y_{n-1}\ldots y_1y_0\rangle \\ |x\rangle &= |x_{n-1}\ldots x_1x_0\rangle \\ |\bar{y}\rangle &= |\bar{y}_{n-1}\ldots\bar{y}_1\bar{y}_0\rangle = \left|2^n-1-y\right\rangle \\ |\bar{x}\rangle &= |\bar{x}_{n-1}\ldots\bar{x}_1\bar{x}_0\rangle = \left|2^n-1-x\right\rangle \\ \bar{y}_i &= 1-y_i,\ \bar{x}_i = 1-x_i \\ & i=0,1,\ldots,n-1 \end{aligned}$$

The flip transformation operators F_y and F_x are denoted as

$$F_y = I^{\otimes 2}\otimes I^{\otimes q}\otimes I^{\otimes n}\otimes X^{\otimes n} \qquad (21)$$

$$F_x = I^{\otimes 2}\otimes I^{\otimes q}\otimes X^{\otimes n}\otimes I^{\otimes n} \qquad (22)$$

The quantum circuits of the flipping transform operators F_y and F_x are shown in Figures 12 and 13.

Theorem 3: The complexity of the quantum gates needed for the flip transformation operators F_y and F_x on the quantum image QIRHSI is $O\left(n\right)$.

Proof of Theorem 3: The flip operators F_y and F_x are shown in Eqs. (21) and (22), and it can be seen that both operators F_y and F_x use n NOT gates, so the complexity of

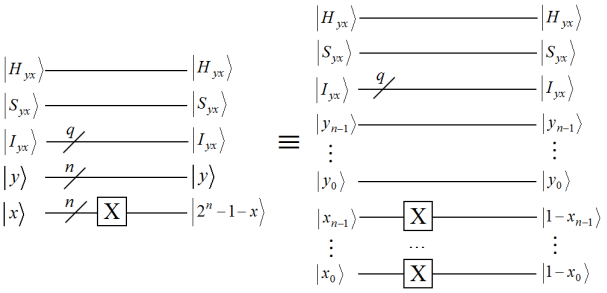

FIGURE 12. QIRHSI color image of the quantum circuit flipped along the *y*-axis.

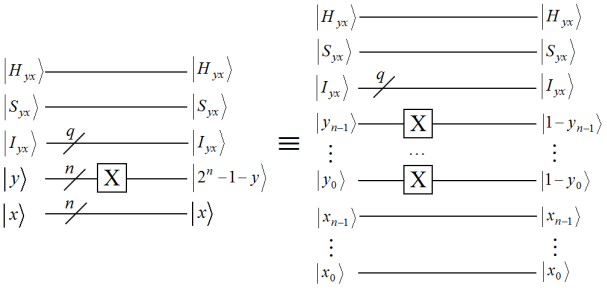

FIGURE 13. QIRHSI color image of the quantum circuit flipped along the *x*-axis.

the quantum gates required to implement the flip operators F_y and F_x on the QIRHSI image is $O\left(n\right)$.

The QIRHSI image is flip transformed along the $y=x$ and $y=-x$ axis as shown in Definition 4. Figure 14 shown an example of the image flipping transformation along the $y=x$ and $y=-x$ axis.

(a) Original Tree image (b) Flipped along the $y=x$ axis (c) Flipped along the $y=-x$ axis

FIGURE 14. The image Tree is transformed by flipping along the $y=x$ and $y=-x$ axis.

Definition 4: The QIRHSI color image based flipping operators $F_{y=x}$ and $F_{y=-x}$ along the $y=x$ and $y=-x$ axis respectively are defined as

$$\begin{aligned} &F_{y=x}\left(|I\left(\theta\right)\rangle\right) \\ &= \frac{1}{2^n}\sum_{y=0}^{2^n-1}\sum_{x=0}^{2^n-1}\left|H_{yx}\right\rangle\left|S_{yx}\right\rangle\left|I_{yx}\right\rangle\otimes V\left(|yx\rangle\right) \\ &= \frac{1}{2^n}\sum_{y=0}^{2^n-1}\sum_{x=0}^{2^n-1}\left|H_{yx}\right\rangle\left|S_{yx}\right\rangle\left|I_{yx}\right\rangle\otimes|xy\rangle \qquad (23) \\ &F_{y=-x}\left(|I\left(\theta\right)\rangle\right) \end{aligned}$$

$$= \frac{1}{2^n}\sum_{y=0}^{2^n-1}\sum_{x=0}^{2^n-1}\left|H_{yx}\right\rangle\left|S_{yx}\right\rangle\left|I_{yx}\right\rangle\otimes\left|\bar{x}\bar{y}\right\rangle$$
$$= \frac{1}{2^n}\sum_{y=0}^{2^n-1}\sum_{x=0}^{2^n-1}\left|H_{yx}\right\rangle\left|S_{yx}\right\rangle\left|I_{yx}\right\rangle\otimes\left|2^n-1-x, 2^n-1-y\right\rangle \tag{24}$$

whereby $|I(\theta)\rangle$ represents a QIRHSI color image, see Eq. (1). The flip transformation operators $F_{y=x}$ and $F_{y=-x}$ can be expressed respectively as

$$F_{y=x} = I^{\otimes 2}\otimes I^{\otimes q}\otimes V \tag{25}$$
$$F_{y=-x} = F_{y=x}F_yF_x \tag{26}$$

The quantum circuits of the flip transformation operators $F_{y=x}$ and $F_{y=-x}$ are shown in Figures 15 and 16, and the quantum circuit of the operator V is given in Figure 17.

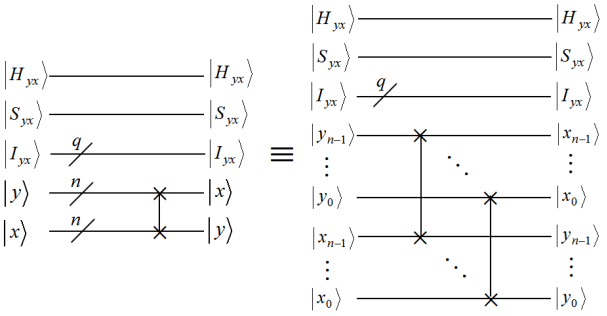

FIGURE 15. QIRHSI image of a flipped quantum circuit along the $y = x$ axis.

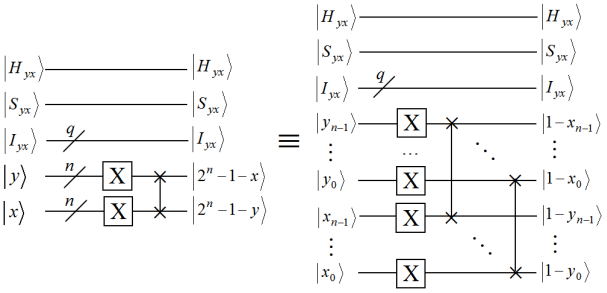

FIGURE 16. QIRHSI image of a flipped quantum circuit along the $y = -x$ axis.

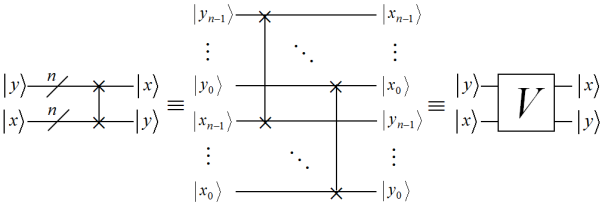

FIGURE 17. Quantum circuits of the operator V.

Theorem 4: The complexity of the quantum gates needed for the flipping operators $F_{y=x}$ and $F_{y=-x}$ on the quantum image QIRHSI is $O(n)$.

Proof of Theorem 4: The flipping operators $F_{y=x}$ and $F_{y=-x}$ are shown in Eqs. (25) and (26), which show that the operator $F_{y=x}$ uses n swap gates, and the operator $F_{y=-x}$ uses $2n$ NOT gates and n swap gates. Because one swap gate is equivalent to three CNOT gates [1], the complexity of the quantum gates needed to implement the flipping operators $F_{y=x}$ and $F_{y=-x}$ on the QIRHSI is $O(n)$.

D. RIGHT-ANGLE ROTATIONS

The transformation of the QIRHSI image rotation angle to $\pi/2$, π and $3\pi/2$ are shown in Definition 5. Figure 18 shows an example of the transformation with image rotation angles $\pi/2$, π and $3\pi/2$.

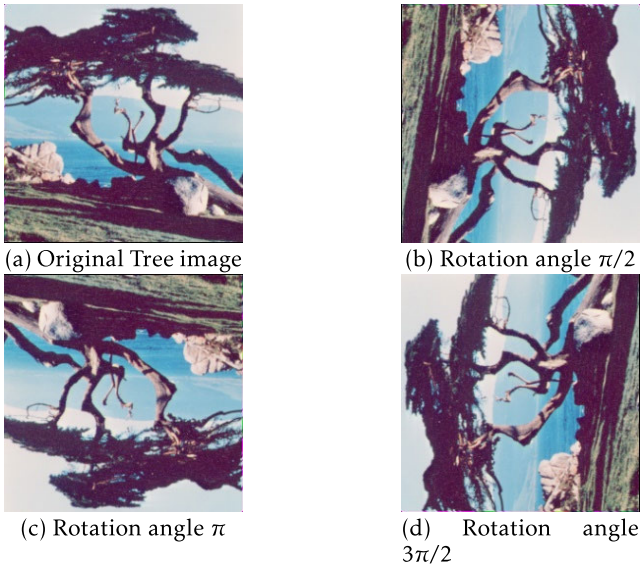

FIGURE 18. Image Tree and right angle after rotation.

Definition 5: The right angle rotation operators $R_{\pi/2}$, R_π and $R_{3\pi/2}$ based on QIRHSI color image rotation angles of $\pi/2$, π and $3\pi/2$ transformations are defined as

$$R_{\pi/2}(|I(\theta)\rangle)$$
$$= \frac{1}{2^n}\sum_{y=0}^{2^n-1}\sum_{x=0}^{2^n-1}\left|H_{yx}\right\rangle\left|S_{yx}\right\rangle\left|I_{yx}\right\rangle\otimes\left|x\bar{y}\right\rangle$$
$$= \frac{1}{2^n}\sum_{y=0}^{2^n-1}\sum_{x=0}^{2^n-1}\left|H_{yx}\right\rangle\left|S_{yx}\right\rangle\left|I_{yx}\right\rangle\otimes\left|x, 2^n-1-y\right\rangle \tag{27}$$
$$R_{\pi}(|I(\theta)\rangle)$$
$$= \frac{1}{2^n}\sum_{y=0}^{2^n-1}\sum_{x=0}^{2^n-1}\left|H_{yx}\right\rangle\left|S_{yx}\right\rangle\left|I_{yx}\right\rangle\otimes\left|\bar{y}\bar{x}\right\rangle$$

$$= \frac{1}{2^n}\sum_{y=0}^{2^n-1}\sum_{x=0}^{2^n-1}\left|H_{yx}\right\rangle\left|S_{yx}\right\rangle\left|I_{yx}\right\rangle\otimes\left|2^n-1-y,2^n-1-x\right\rangle \tag{28}$$

$$R_{3\pi/2}\left(\left|I\left(\theta\right)\right\rangle\right)$$
$$= \frac{1}{2^n}\sum_{y=0}^{2^n-1}\sum_{x=0}^{2^n-1}\left|H_{yx}\right\rangle\left|S_{yx}\right\rangle\left|I_{yx}\right\rangle\otimes\left|\bar{x}y\right\rangle$$
$$= \frac{1}{2^n}\sum_{y=0}^{2^n-1}\sum_{x=0}^{2^n-1}\left|H_{yx}\right\rangle\left|S_{yx}\right\rangle\left|I_{yx}\right\rangle\otimes\left|2^n-1-x,y\right\rangle \tag{29}$$

where $|I(\theta)\rangle$ represents a QIRHSI color image, see Eq. (1). The right-angle rotation operators $R_{\pi/2}$, R_π and $R_{3\pi/2}$ can be expressed respectively as

$$R_{\pi/2} = F_{y=x}F_x \tag{30}$$
$$R_\pi = F_yF_x \tag{31}$$
$$R_{3\pi/2} = F_{y=x}F_y \tag{32}$$

The quantum circuits of the operators $R_{\pi/2}$, R_π and $R_{3\pi/2}$ are shown in Figures 19, 20 and 21.

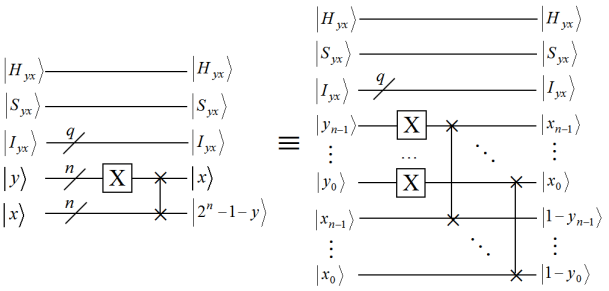

FIGURE 19. QIRHSI image of the quantum circuit with a rotation angle of $\pi/2$.

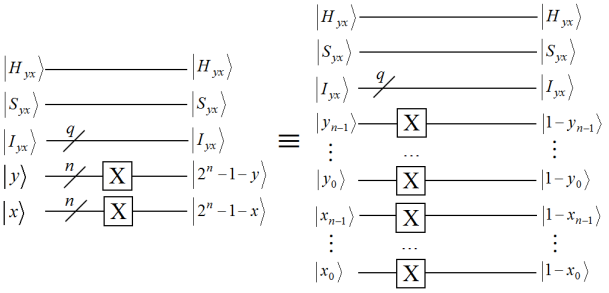

FIGURE 20. QIRHSI image of the quantum circuit with a rotation angle of π.

Theorem 5: The complexity of the quantum gates required for the right-angle rotation operators $R_{\pi/2}$, R_π and $R_{3\pi/2}$ on the quantum image QIRHSI is $O(n)$.

Proof of Theorem 5: The right-angle rotation operators $R_{\pi/2}$, R_π and $R_{3\pi/2}$ are shown in Eqs. (30), (31) and (32), and it can be known that the operator $R_{\pi/2}$ uses n NOT gates and n swap gates, the operator R_π uses n NOT gates, and the operator $R_{3\pi/2}$ uses n NOT gates and n swap gates. Thus, the complexity of the quantum gates needed to implement the right-angle rotation operators $R_{\pi/2}$, R_π and $R_{3\pi/2}$ on the QIRHSI is $O(n)$.

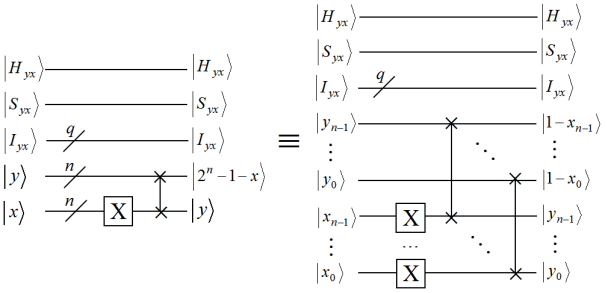

FIGURE 21. QIRHSI image of the quantum circuit with a rotation angle of $3\pi/2$.

IV. COMPARISON OF THE COMPLEXITY OF QUANTUM GEOMETRIC TRANSFORMATIONS

The geometric transformation of quantum images has been a highly interesting research topic for scholars. As yet, geometric transformations based on the two-dimensional quantum gray-scale image FRQI [24] and geometric transformations based on the multidimensional quantum color image NASS [26] are the two ways that can be used. Table 2 gives the complexity of the quantum gates needed for the geometric transformation operations based on the quantum image representation models FRQI, NASS and QIRHSI. It was indicated that this table compares images of size $2^n \times 2^n$.

TABLE 2. The complexity of the quantum gates required for geometric transformations based on different quantum image models is compared.

Geometric transformations	Based on QIRHSI representation	Based on NASS representation	Based on FRQI representation
Two-point swap	$O\left(n^2\right)$	$O\left(n^2\right)$	$O\left(n^2\right)$
Circular translations	$O(n)$	$O\left(2^n n^2\right)$	–
Flip transformations	$O(n)$	$O(n)$	$O(n)$
Right-angle rotations	$O(n)$	$O(n)$	$O(n)$

As can be seen from Table 2, the quantum gray-scale image FRQI involved no circular translation, while the complexity $O(n)$ of quantum gates required for the quantum circular translation operation designed in this paper based on the quantum 2D color image QIRHSI is much lower than the complexity $O\left(2^n n^2\right)$ of the quantum circular translation operation designed based on the quantum multi-dimensional color image NASS.

In classical computers, the global operators of geometric transformations require 2^{2n} matrices to be implemented, therefore the complexity of the implemented operations are

at least $O\left(2^{2n}\right)$. However, in quantum systems, no matter for quantum image representation FRQI, NASS and QIRHSI, quantum global transform operations (circular translation, flipping transform and right-angle rotation) require less complexity of quantum gates than local transform operations (two-point swapping), which are required to be implemented by $O(n)$ quantum gates, and the reason for this result is due to the parallelism of quantum computing. Therefore, quantum geometric transformation techniques based on quantum image representation FRQI, NASS and QIRHSI are applied to image encryption [70], [81], watermarking [47] and so on.

V. EXPERIMENTAL EXAMPLE OF THE QIRHSI GEOMETRIC TRANSFORMATIONS

In order to make the geometric transformation based on the QIRHSI image more visual, a quantum color image QIRHSI of size 4×4, where $n = 2$ and $q = 8$, is shown in Figure 22 as an example. A 4×4 color image of QIRHSI is given in Figure 22 and is represented in Eq. (33).

$$\begin{aligned} |I(\theta)\rangle &= \frac{1}{2^2}\sum_{k=0}^{2^4-1}|H_k\rangle|S_k\rangle|I_k\rangle \otimes |k\rangle \\ &= \frac{1}{4}\sum_{y=0}^{2^2-1}\sum_{x=0}^{2^2-1}\left|H_{yx}\right\rangle\left|S_{yx}\right\rangle\left|I_{yx}\right\rangle \otimes |yx\rangle \end{aligned} \tag{33}$$

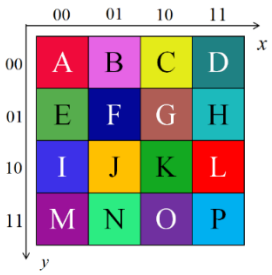

FIGURE 22. A 4 × 4 color image of QIRHSI.

A. TWO-POINT SWAP

Figure 23 gives an example of a QIRHSI color image where two pixels $|i\rangle = |1\rangle = |00\rangle|01\rangle$ and $|j\rangle = |11\rangle = |10\rangle|11\rangle$ are swapped. The corresponding quantum circuits are given in Figure 24. The two-point swap operator G_P is defined as

$$\begin{aligned} G_P &= I^{\otimes 2} \otimes I^{\otimes 8} \otimes P \\ &= I^{\otimes 2} \otimes I^{\otimes 8} \otimes \left\{ \begin{array}{l} |1\rangle\langle 11| + |11\rangle\langle 1| + \\ \sum_{k=0,k\neq 1,11}^{15} |k\rangle\langle k| \end{array} \right\} \end{aligned} \tag{34}$$

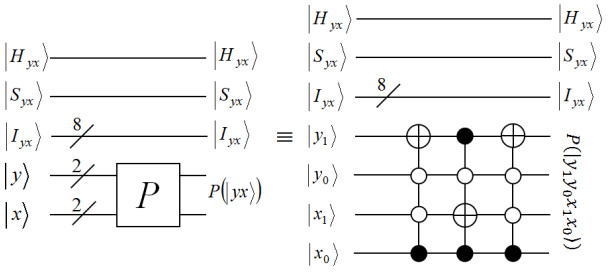

FIGURE 24. The quantum circuit for two-point swapping.

Applying Eq. (34) to image $|I(\theta)\rangle$ gives

$$\begin{aligned} &G_P(|I(\theta)\rangle) \\ &= \frac{1}{4}\sum_{k=0}^{15}|H_k\rangle|S_k\rangle|I_k\rangle \otimes P(|k\rangle) \\ &= \frac{1}{4}\left\{ \begin{array}{l} |H_{11}\rangle|S_{11}\rangle|I_{11}\rangle \otimes |1\rangle + |H_1\rangle|S_1\rangle|I_1\rangle \otimes |11\rangle \\ + \sum_{k=0,k\neq 1,11}^{15} |H_k\rangle|S_k\rangle|I_k\rangle \otimes |k\rangle \end{array} \right\} \end{aligned}$$

where $P(|k\rangle) = |k\rangle$, $k \neq 1$, 11, and $P(|1\rangle) = |11\rangle$, $P(|11\rangle) = |1\rangle$.

Observing Figure 23, it can be seen that we swapped the two pixels labeled with the alphabets B and L, corresponding to the pixel positions 1 and 11, respectively. From the quantum circuit shown in Figure 24, it can be seen that swapping pixel positions 1 and 11 requires six NOT gates and three controlled not-gates. Since one three-controlled not-gate is equivalent to four Toffoli gates, one Toffoli gate is equivalent to six controlled not-gates. Therefore, swapping pixel locations 1 and 11 needs six NOT gates and 72 controlled not-gates.

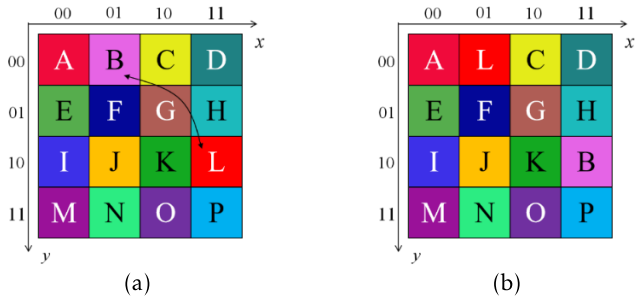

FIGURE 23. (a) Original image; (b) After the two-point swap.

B. CIRCULAR TRANSLATION

An example of circular translation of a QIRHSI color image along the x-axis is given in Figure 25, where $l = 3$. The corresponding quantum circuit are given in Figure 26. The circular translation operator T_{x+3} is defined as

$$\begin{aligned} T_{x+3} &= I^{\otimes 2} \otimes I^{\otimes 8} \otimes I^{\otimes 2} \otimes \sum_{j=0}^{3} |(j+3) \bmod 4\rangle\langle j| \\ &= I^{\otimes 2} \otimes I^{\otimes 8} \otimes I^{\otimes 2} \\ &\quad \otimes (|3\rangle\langle 0| + |0\rangle\langle 1| + |1\rangle\langle 2| + |2\rangle\langle 3|) \end{aligned}$$

Applying the circular translation operator T_{x+3} to the image $|I(\theta)\rangle$ to obtain

$$T_{x+3}(|I(\theta)\rangle) = \frac{1}{4}\sum_{y=0}^{3}\sum_{x=0}^{3}|H_{yx}\rangle|S_{yx}\rangle|I_{yx}\rangle \otimes |y, (x+3)\ mod\ 4\rangle$$

Obviously, it is a circular translation of Figure 22 by 3 pixels along the positive direction of the x-axis to obtain Figure 25(b). Analysis of the quantum circuit shown in Figure 26 shows that the use of a module 4 adder is equivalent to the use of 5 plain, 2 NOT gates and no more than 8 controlled not-gates (See Theorem 2). In other words, the circular translation of 3 pixels along the positive direction of the x-axis uses 5 NOT gates and 228 controlled not-gates.

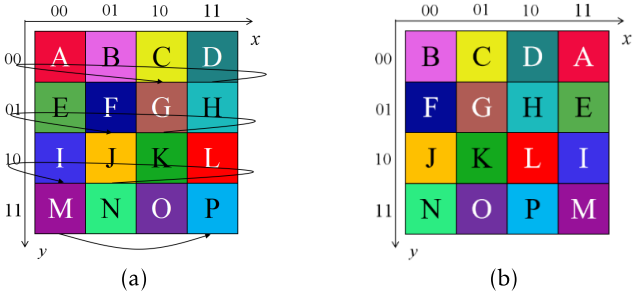

FIGURE 25. (a) Original image; (b) After circular translation.

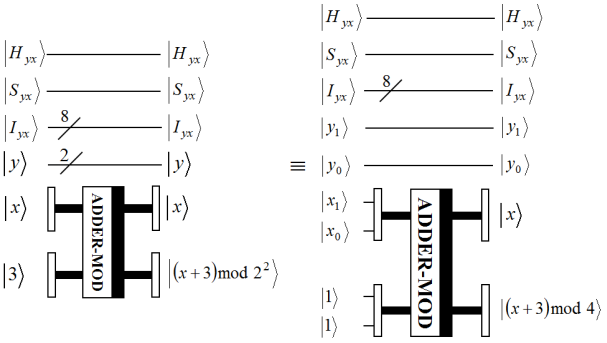

FIGURE 26. Quantum circuits of circular translations.

C. FLIP TRANSFORMATION

Figure 27 gives an example of a QIRHSI color image flipped along the x axis. The corresponding quantum circuits are shown in Figure 28.

The flip transformation operator F_x is described by the definition of

$$F_x = I^{\otimes 2} \otimes I^{\otimes 8} \otimes X^{\otimes 2} \otimes I^{\otimes 2}$$

Applying the flip transformation operator F_x to the image $|I(\theta)\rangle$ gives

$$F_x(|I(\theta)\rangle) = \frac{1}{4}\sum_{y=0}^{3}\sum_{x=0}^{3}|H_{yx}\rangle|S_{yx}\rangle|I_{yx}\rangle \otimes |3-y, x\rangle$$

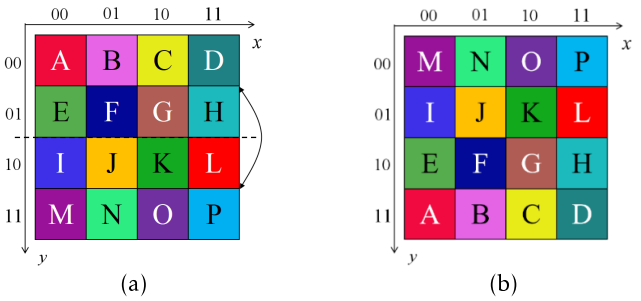

FIGURE 27. (a) Original image; (b) After the flip transformation.

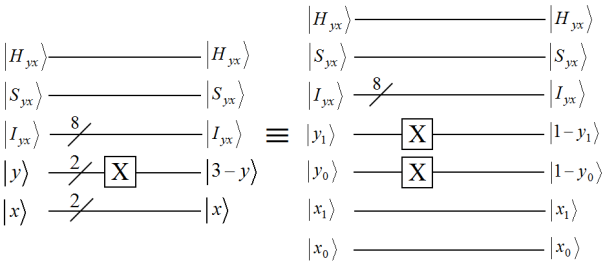

FIGURE 28. The quantum circuit of the flip transformation along the x axis.

Obviously, a flipping transformation of Figure 22 along the x-axis to obtain Figure 27(b) requires only 2 NOT gates (see Figure 28).

D. FLIP TRANSFORMATION

An example of a QIRHSI color image flipped transformation along the $y = x$ axis is given in Figure 29. Figure 30 gives the corresponding quantum circuits.

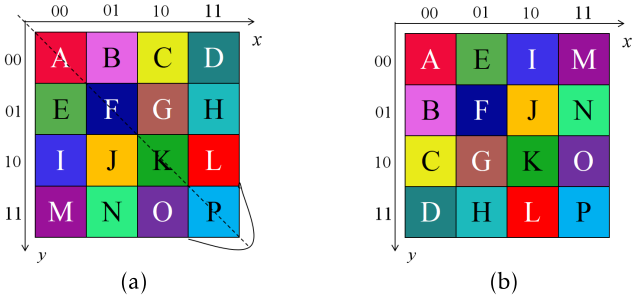

FIGURE 29. (a) Original image; (b) After flipping along the $y = x$ axis.

The flip transformation operator $F_{y=x}$ defined as

$$F_{y=x} = I^{\otimes 2} \otimes I^{\otimes 8} \otimes V$$

where the operator V is shown in Figure 31.

The flip transformation operator $F_{y=x}$ is applied to the image $|I(\theta)\rangle$ to obtain

$$F_{y=x}(|I(\theta)\rangle) = \frac{1}{4}\sum_{y=0}^{3}\sum_{x=0}^{3}|H_{yx}\rangle|S_{yx}\rangle|I_{yx}\rangle \otimes |xy\rangle$$

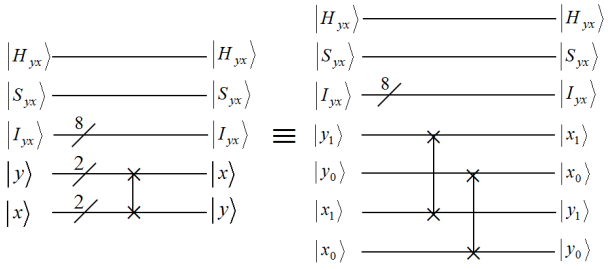

FIGURE 30. The quantum circuit flipped along the $y = x$ axis.

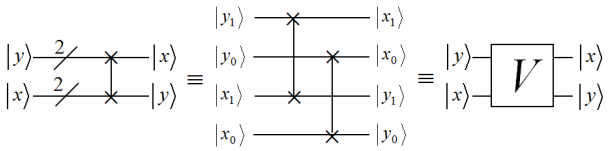

FIGURE 31. Quantum circuit of the operator V.

The flipping transformation of Figure 22 along the $y = x$ axis results in Figure 29(b), which requires only two swap gates to complete the operation (see Figure 30). One swap gate is equivalent to three controlled not-gates. Therefore, six controlled not-gates are needed for the flipping transformation operation along the $y = x$ axis.

E. RIGHT-ANGLE ROTATION

An example of a QIRHSI color image rotated an angle of $\pi/2$ is given in Figure 32. The corresponding quantum circuits are provided in Figure 33. The right-angle rotation operator $R_{\pi/2}$ is

$$R_{\pi/2} = F_{y=x} F_x$$

Applying the right-angle rotation operator $R_{\pi/2}$ to the image $|I(\theta)\rangle$ gives

$$R_{\pi/2}(|I(\theta)\rangle) = \frac{1}{4}\sum_{y=0}^{3}\sum_{x=0}^{3}|H_{yx}\rangle|S_{yx}\rangle|I_{yx}\rangle \otimes |x, 3-y\rangle$$

Rotating Figure 22 by $\pi/2$ to obtain Figure 32(b), only two NOT gates and two swap gates are needed (see Figure 33), i.e., only two NOT gates and six controlled not-gates are needed to complete this operation.

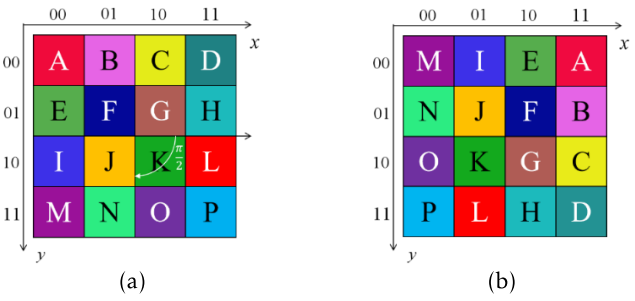

FIGURE 32. (a) Original image; (b) After rotation $\pi/2$.

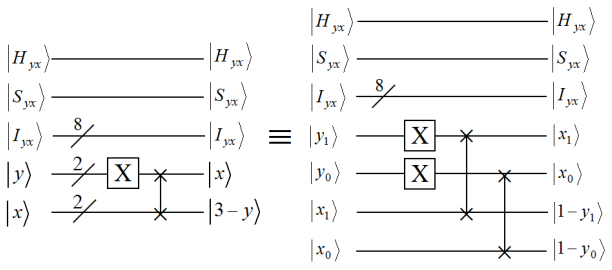

FIGURE 33. The quantum circuit of rotated $\pi/2$.

VI. DISCUSSIONS

This paper presents geometric transformations (two-point swapping, circular translation, flip transformation and right-angle rotation) based on quantum color image QIRHSI. However, there are not enough geometric transformations in the above mentioned methods. Firstly, we cannot verify the above algorithm directly on a quantum computer under the current conditions. Secondly, it only gives the algorithm and quantum circuit for circular translation, and not for general translation. Finally, the flip transformation and right-angle rotation are only designed for some special types of transformations, and their applications are limited.

VII. CONCLUSION AND FUTURE OUTLOOK

In this paper, quantum geometric transformations based on the quantum color image QIRHSI are proposed, covering two-point swapping, circular translation, flipping transformations and right-angle rotation. The quantum circuits for the four types of geometric transformation operations mentioned above are designed immediately afterwards, and the complexity analysis of the quantum gates needed for the different types of geometric transformation unitary operators are given. The complexity of the global transformation (circular translation, flipping transformation and right-angle rotation) operator of the quantum color image QIRHSI is lower than with the local transformation (two-point swapping) operator. Finally, the quantum geometric transformation operation of QIRHSI color image is illustrated by a simple 4×4 example.

The future research work covers:

1) The circular transformations, flipping transformations and right-angle rotations covered in this paper are whole geometric transformations, and it is essential to implement local circular translations, local flipping transformations and local right-angle rotations.
2) Flipping transformations (along the y axis, x axis, $y = x$ axis and $y = -x$ axis) and right-angle rotations ($\pi/2$, π and $3\pi/2$) are both special quantum geometric transformations and how to design flipping transformations along the arbitrary axis and rotating transformations at arbitrary angles.
3) How to design general translation operations in the field of quantum image processing after designing circular translation operations with modulo N adder.

4) How to construct arbitrary geometric transformations using the two-point swapping operator, while making the designed quantum circuits for arbitrary geometric transformations with lower complexity is still a problem to be further considered.
5) Additional applications in quantum image processing combined with quantum geometric transformations are of higher value, for example, in quantum image encryption, where pixel position scrambling in quantum image encryption can be accomplished by combining sequences generated by chaotic mapping with quantum circuits.
6) In practical applications, how to better use quantum geometric transformations to correction of images taken by artificial satellites and how to use quantum geometric transformations to processing satellite cloud images commonly used in weather forecast, etc.

ACKNOWLEDGMENT

The authors would like to acknowledge Prince Sultan University for paying the Article Processing Charges (APC) of this publication.

REFERENCES

[1] M. A. Nielsen and I. L. Chuang, *Quantum Computation and Quantum Information*. Cambridge, U.K.: Cambridge Univ. Press, 2010.
[2] R. P. Feynman, "Simulating physics with computers," *Int. J. Theor. Phys.*, vol. 21, nos. 6–7, pp. 467–488, 1982.
[3] P. W. Shor, "Algorithms for quantum computation: Discrete logarithms and factoring," in *Proc. 35th Annu. Symp. Found. Comput. Sci.*, 1994, pp. 124–134.
[4] L. K. Grover, "A fast quantum mechanical algorithm for database search," in *Proc. 28th Annu. ACM Symp. Theory Comput.*, 1996, pp. 212–219.
[5] S. E. Venegas-Andraca and S. Bose, "Storing, processing, and retrieving an image using quantum mechanics," *Proc. SPIE*, vol. 5105, pp. 137–147, Aug. 2003.
[6] J. I. Latorre, "Image compression and entanglement," *Quantum Phys.*, pp. 1–4, Oct. 2005. [Online]. Available: https://arxiv.53yu.com/abs/quant-ph/0510031
[7] S. E. Venegas-Andraca and J. L. Ball, "Processing images in entangled quantum systems," *Quantum Inf. Process.*, vol. 9, no. 1, pp. 1–11, Feb. 2010.
[8] P. Q. Le, F. Dong, and K. Hirota, "A flexible representation of quantum images for polynomial preparation, image compression, and processing operations," *Quantum Inf. Process.*, vol. 10, no. 1, pp. 63–84, 2012.
[9] B. Sun, P. Q. Le, A. M. Iliyasu, F. Yan, J. A. Garcia, F. Dong, and K. Hirota, "A multi-channel representation for images on quantum computers using the RGBα color space," in *Proc. IEEE 7th Int. Symp. Intell. Signal Process.*, Sep. 2011, pp. 19–21.
[10] Y. Zhang, K. Lu, Y. Gao, and M. Wang, "NEQR: A novel enhanced quantum representation of digital images," *Quantum Inf. Process.*, vol. 12, no. 8, pp. 2833–2860, 2013.
[11] H.-S. Li, Q. Zhu, R.-G. Zhou, L. Song, and X.-J. Yang, "Multi-dimensional color image storage and retrieval for a normal arbitrary quantum superposition state," *Quantum Inf. Process.*, vol. 13, no. 4, pp. 991–1011, 2014.
[12] X. Song, S. Wang, and X. Niu, "Multi-channel quantum image representation based on phase transform and elementary transformations," *J. Inf. Hiding Multimedia Signal Process.*, vol. 5, no. 4, pp. 574–585, 2014.
[13] Y.-G. Yang, X. Jia, S.-J. Sun, and Q.-X. Pan, "Quantum cryptographic algorithm for color images using quantum Fourier transform and double random-phase encoding," *Inf. Sci.*, vol. 277, pp. 445–457, Sep. 2014.
[14] S. Yuan, X. Mao, Y. Xue, L. Chen, Q. Xiong, and A. Compare, "SQR: A simple quantum representation of infrared images," *Quantum Inf. Process.*, vol. 13, no. 6, pp. 1353–1379, 2014.
[15] N. Jiang, J. Wang, and Y. Mu, "Quantum image scaling up based on nearest-neighbor interpolation with integer scaling ratio," *Quantum Inf. Process.*, vol. 14, no. 11, pp. 4001–4026, Nov. 2015.
[16] J. Sang, S. Wang, and Q. Li, "A novel quantum representation of color digital images," *Quantum Inf. Process.*, vol. 16, no. 2, pp. 1–14, Feb. 2017.
[17] H.-S. Li, X. Chen, H. Xia, Y. Liang, and Z. Zhou, "A quantum image representation based on bitplanes," *IEEE Access*, vol. 6, pp. 62396–62404, 2018.
[18] G. Xu, X. Xu, X. Wang, and X. Wang, "Order-encoded quantum image model and parallel histogram specification," *Quantum Inf. Process.*, vol. 18, no. 11, pp. 1–26, Nov. 2019.
[19] L. Wang, Q. Ran, J. Ma, S. Yu, and L. Tan, "QRCI: A new quantum representation model of color digital images," *Opt. Commun.*, vol. 438, pp. 147–158, May 2019.
[20] A. M. Grigoryan and S. S. Agaian, "New look on quantum representation of images: Fourier transform representation," *Quantum Inf. Process.*, vol. 19, no. 5, pp. 1–26, May 2020.
[21] F. Yan, N. Li, and K. Hirota, "QHSL: A quantum hue, saturation, and lightness color model," *Inf. Sci.*, vol. 577, pp. 196–213, Oct. 2021.
[22] G.-L. Chen, X.-H. Song, S. E. Venegas-Andraca, and A. A. A. El-Latif, "QIRHSI: Novel quantum image representation based on HSI color space model," *Quantum Inf. Process.*, vol. 21, no. 1, pp. 1–31, Jan. 2022.
[23] M. Lisnichenko and S. Protasov, "Quantum image representation: A review," *Quantum Mach. Intell.*, vol. 5, no. 1, pp. 1–2, Jun. 2023.
[24] P. Q. Le, A. M. Iliyasu, F. Dong, and K. Hirota, "Fast geometric transformations on quantum images," *IAENG Int. J. Appl. Math.*, vol. 40, no. 3, pp. 1–2, 2010.
[25] P. Q. Le, A. M. Iliyasu, F. Dong, and K. Hirota, "Strategies for designing geometric transformations on quantum images," *Theor. Comput. Sci.*, vol. 412, pp. 1406–1418, Mar. 2011.
[26] P. Fan, R.-G. Zhou, N. Jing, and H.-S. Li, "Geometric transformations of multidimensional color images based on NASS," *Inf. Sci.*, vols. 340–341, pp. 191–208, May 2016.
[27] F. Yan, K. Chen, S. E. Venegas-Andraca, and J. Zhao, "Quantum image rotation by an arbitrary angle," *Quantum Inf. Process.*, vol. 16, no. 11, p. 282, Nov. 2017.
[28] J. Wang, N. Jiang, and L. Wang, "Quantum image translation," *Quantum Inf. Process.*, vol. 14, no. 5, pp. 1589–1604, May 2015.
[29] R.-G. Zhou, C. Tan, and H. Ian, "Global and local translation designs of quantum image based on FRQI," *Int. J. Theor. Phys.*, vol. 56, no. 4, pp. 1382–1398, Apr. 2017.
[30] N. Jiang and L. Wang, "Quantum image scaling using nearest neighbor interpolation," *Quantum Inf. Process.*, vol. 14, no. 5, pp. 1559–1571, 2015.
[31] J. Sang, S. Wang, and X. Niu, "Quantum realization of the nearest-neighbor interpolation method for FRQI and NEQR," *Quantum Inf. Process.*, vol. 15, no. 1, pp. 37–64, Jan. 2016.
[32] P. Li and X. Liu, "Bilinear interpolation method for quantum images based on quantum Fourier transform," *Int. J. Quantum Inf.*, vol. 16, no. 4, Jun. 2018, Art. no. 1850031.
[33] R.-G. Zhou, Y. Cheng, X. Qi, H. Yu, and N. Jiang, "Asymmetric scaling scheme over the two dimensions of a quantum image," *Quantum Inf. Process.*, vol. 19, no. 9, p. 343, Sep. 2020.
[34] P. Q. Le, A. M. Iliyasu, F. Dong, and K. Hirota, "Efficient color transformations on quantum images," *J. Adv. Comput. Intell. Intell. Inform.*, vol. 15, no. 6, pp. 698–706, 2011.
[35] N. Jiang, W.-Y. Wu, and L. Wang, "The quantum realization of Arnold and Fibonacci image scrambling," *Quantum Inf. Process.*, vol. 13, no. 5, pp. 1223–1236, May 2014.
[36] N. Jiang and L. Wang, "Analysis and improvement of the quantum Arnold image scrambling," *Quantum Inf. Process.*, vol. 13, no. 7, pp. 1545–1551, Jul. 2014.
[37] N. Jiang, L. Wang, and W.-Y. Wu, "Quantum Hilbert image scrambling," *Int. J. Theor. Phys.*, vol. 53, no. 7, pp. 2463–2484, 2014.
[38] R.-G. Zhou, Y.-J. Sun, and P. Fan, "Quantum image gray-code and bit-plane scrambling," *Quantum Inf. Process.*, vol. 14, no. 5, pp. 1717–1734, 2015.
[39] S. Caraiman and V. I. Manta, "Image segmentation on a quantum computer," *Quantum Inf. Process.*, vol. 14, no. 5, pp. 1693–1715, May 2015.
[40] P. Li, T. Shi, Y. Zhao, and A. Lu, "Design of threshold segmentation method for quantum image," *Int. J. Theor. Phys.*, vol. 59, no. 2, pp. 514–538, Feb. 2020.

[41] S. Yuan, C. Wen, B. Hang, and Y. Gong, "The dual-threshold quantum image segmentation algorithm and its simulation," *Quantum Inf. Process.*, vol. 19, no. 12, p. 425, Dec. 2020.

[42] Y. Zhang, K. Lu, K. Xu, Y. Gao, and R. Wilson, "Local feature point extraction for quantum images," *Quantum Inf. Process.*, vol. 14, no. 5, pp. 1573–1588, May 2015.

[43] N. Jiang, Z. Ji, H. Li, and J. Wang, "Quantum image interest point extraction," *Mod. Phys. Lett. A*, vol. 36, no. 9, Mar. 2021, Art. no. 2150063.

[44] W.-W. Zhang, F. Gao, B. Liu, H.-Y. Jia, Q.-Y. Wen, and H. Chen, "A quantum watermark protocol," *Int. J. Theor. Phys.*, vol. 52, no. 2, pp. 504–513, Feb. 2013.

[45] A. M. Iliyasu, P. Q. Le, F. Dong, and K. Hirota, "Watermarking and authentication of quantum images based on restricted geometric transformations," *Inf. Sci.*, vol. 186, no. 1, pp. 126–149, 2012.

[46] Y.-G. Yang, X. Jia, P. Xu, and J. Tian, "Analysis and improvement of the watermark strategy for quantum images based on quantum Fourier transform," *Quantum Inf. Process.*, vol. 12, no. 8, pp. 2765–2769, Aug. 2013.

[47] X.-H. Song, S. Wang, S. Liu, A. A. A. El-Latif, and X.-M. Niu, "A dynamic watermarking scheme for quantum images using quantum wavelet transform," *Quantum Inf. Process.*, vol. 12, no. 12, pp. 3689–3706, 2013.

[48] F. Yan, A. M. Iliyasu, B. Sun, S. E. Venegas-Andraca, F. Dong, and K. Hirota, "A duple watermarking strategy for multi-channel quantum images," *Quantum Inf. Process.*, vol. 14, no. 5, pp. 1675–1692, 2015.

[49] S. Heidari and M. Naseri, "A novel LSB based quantum watermarking," *Int. J. Theor. Phys.*, vol. 55, no. 10, pp. 4205–4218, 2016.

[50] P. Li, Y. Zhao, H. Xiao, and M. Cao, "An improved quantum watermarking scheme using small-scale quantum circuits and color scrambling," *Quantum Inf. Process.*, vol. 16, no. 5, p. 127, 2017.

[51] Y.-G. Yang, J. Xia, X. Jia, and H. Zhang, "Novel image encryption/decryption based on quantum Fourier transform and double phase encoding," *Quantum Inf. Process.*, vol. 12, no. 11, pp. 3477–3493, 2013.

[52] D. Awasthi and V. K. Srivastava, "Robust, imperceptible and optimized watermarking of DICOM image using Schur decomposition, LWT-DCT-SVD and its authentication using SURF," *Multimedia Tools Appl.*, vol. 2022, pp. 1–35, Sep. 2022.

[53] S. Iranmanesh, R. Atta, and M. Ghanbari, "Implementation of a quantum image watermarking scheme using NEQR on IBM quantum experience," *Quantum Inf. Process.*, vol. 21, no. 6, p. 194, Jun. 2022.

[54] A. Ullah, A. A. Shah, J. S. Khan, M. Sajjad, W. Boulila, A. Akgul, J. Masood, F. A. Ghaleb, S. A. Shah, and J. Ahmad, "An efficient lightweight image encryption scheme using multichaos," *Secur. Commun. Netw.*, vol. 2022, pp. 1–16, Oct. 2022.

[55] Y. Y. Ghadi, S. A. Alsuhibany, J. Ahmad, H. Kumar, W. Boulila, M. Alsaedi, K. Khan, and S. A. Bhatti, "Multi-chaos-based lightweight image encryption-compression for secure occupancy monitoring," *J. Healthcare Eng.*, vol. 2022, pp. 1–14, Nov. 2022.

[56] F. Ahmed, M. U. Rehman, J. Ahmad, M. S. Khan, W. Boulila, G. Srivastava, J. C.-W. Lin, and W. J. Buchanan, "A DNA based colour image encryption scheme using a convolutional autoencoder," *ACM Trans. Multimedia Comput., Commun., Appl.*, vol. 2022, pp. 1–22, Nov. 2022.

[57] F. Masood, J. Masood, L. Zhang, S. S. Jamal, W. Boulila, S. U. Rehman, F. A. Khan, and J. Ahmad, "A new color image encryption technique using DNA computing and Chaos-based substitution box," *Soft Comput.*, vol. 26, pp. 1–17, Apr. 2021.

[58] T. Hua, J. Chen, D. Pei, W. Zhang, and N. Zhou, "Quantum image encryption algorithm based on image correlation decomposition," *Int. J. Theor. Phys.*, vol. 54, pp. 526–537, Feb. 2015.

[59] N. R. Zhou, T. X. Hua, L. H. Gong, D. J. Pei, and Q. H. Liao, "Quantum image encryption based on generalized Arnold transform and double random-phase encoding," *Quantum Inf. Process.*, vol. 14, no. 4, pp. 1193–1213, 2015.

[60] L.-H. Gong, X.-T. He, S. Cheng, T.-X. Hua, and N.-R. Zhou, "Quantum image encryption algorithm based on quantum image XOR operations," *Int. J. Theor. Phys.*, vol. 55, no. 7, pp. 3234–3250, Jul. 2016.

[61] L. Li, B. Abd-El-Atty, A. A. El-Latif, and A. Ghoneim, "Quantum color image encryption based on multiple discrete chaotic systems," in *Proc. Federated Conf. Comput. Sci. Inf. Syst.*, Sep. 2017, pp. 3–6.

[62] L.-H. Gong, X.-T. He, R.-C. Tan, and Z.-H. Zhou, "Single channel quantum color image encryption algorithm based on HSI model and quantum Fourier transform," *Int. J. Theor. Phys.*, vol. 57, no. 1, pp. 59–73, Jan. 2018.

[63] Q. W. Ran, S. Yu, L. Wang, and J. Ma, "A quantum color image encryption scheme based on coupled hyper-chaotic Lorenz system with three impulse injections," *Quantum Inf. Process.*, vol. 17, no. 8, p. 188, 2018.

[64] A. A. A. El-Latif, B. Abd-El-Atty, S. E. Venegas-Andraca, and W. Mazurczyk, "Efficient quantum-based security protocols for information sharing and data protection in 5G networks," *Future Gener. Comput. Syst.*, vol. 100, pp. 893–906, Nov. 2019.

[65] A. A. A. El-Latif, B. Abd-El-Atty, and S. E. Venegas-Andraca, "Controlled alternate quantum walk-based pseudo-random number generator and its application to quantum color image encryption," *Phys. A, Stat. Mech. Appl.*, vol. 547, Jun. 2020, Art. no. 123869.

[66] B. Abd-El-Atty, A. A. Abd El-Latif, and S. E. Venegas-Andraca, "An encryption protocol for NEQR images based on one-particle quantum walks on a circle," *Quantum Inf. Process.*, vol. 18, no. 9, p. 272, Sep. 2019.

[67] X. Liu, D. Xiao, and C. Liu, "Three-level quantum image encryption based on Arnold transform and logistic map," *Quantum Inf. Process.*, vol. 20, no. 1, p. 23, Jan. 2021.

[68] U. Erkan, A. Toktas, and Q. Lai, "2D hyperchaotic system based on Schaffer function for image encryption," *Expert Syst. Appl.*, vol. 213, Mar. 2023, Art. no. 119076.

[69] U. Erkan, A. Toktas, F. Toktas, and F. Alenezid, "2D eπ-map for image encryption," *Inf. Sci.*, vol. 589, pp. 770–789, Apr. 2022.

[70] X. Song, G. Chen, and A. A. A. El-Latif, "Quantum color image encryption scheme based on geometric transformation and intensity channel diffusion," *Mathematics*, vol. 10, no. 17, p. 3038, Aug. 2022.

[71] O. Bryngdahl, "Geometrical transformations in optics," *J. Opt. Soc. Amer.*, vol. 64, no. 8, pp. 1092–1099, 1974.

[72] S. R. Dooley, R. W. Stewart, T. S. Durrani, S. K. Setarehdan, and J. J. Soraghan, "Efficient implementation of accurate geometric transformations for 2-D and 3-D image processing," *IEEE Trans. Image Process.*, vol. 13, no. 8, pp. 1060–1065, Aug. 2004.

[73] E. R. Arce-Santana and A. Alba, "Image registration using Markov random coefficient and geometric transformation fields," *Pattern Recognit.*, vol. 42, no. 8, pp. 1660–1671, 2009.

[74] Y. Zhang, K. Lu, Y. Gao, and K. Xu, "A novel quantum representation for log-polar images," *Quantum Inf. Process.*, vol. 12, no. 9, pp. 3103–3126, 2013.

[75] M. Wang, K. Lu, Y. Zhang, and X. Wang, "FLPI: Representation of quantum images for log-polar coordinate," *Proc. SPIE*, vol. 8878, pp. 21–22, Jul. 2013.

[76] R.-G. Zhou, Q. Wu, M.-Q. Zhang, and C.-Y. Shen, "Quantum image encryption and decryption algorithms based on quantum image geometric transformations," *Int. J. Theor. Phys.*, vol. 52, no. 6, pp. 1802–1817, 2013.

[77] X.-H. Song, S. Wang, A. A. A. El-Latif, and X. M. Niu, "Quantum image encryption based on restricted geometric and color transformations," *Quantum Inf. Process.*, vol. 13, no. 8, pp. 1765–1787, 2014.

[78] V. Vedral, A. Barenco, and A. Ekert, "Quantum networks for elementary arithmetic operations," *Phys. Rev. A, Gen. Phys.*, vol. 54, no. 1, pp. 147–153, Jul. 1996.

[79] F. Orts, G. Ortega, E. F. Combarro, and E. M. Garzón, "A review on reversible quantum adders," *J. Netw. Comput. Appl.*, vol. 170, Nov. 2020, Art. no. 102810.

[80] A. Barenco, C. H. Bennett, R. Cleve, D. P. DiVincenzo, N. Margolus, P. Shor, T. Sleator, J. A. Smolin, and H. Weinfurter, "Elementary gates for quantum computation," *Phys. Rev. A, Gen. Phys.*, vol. 52, no. 5, pp. 3457–3467, 1995.

[81] H.-S. Li, C. Li, X. Chen, and H.-Y. Xia, "Quantum image encryption algorithm based on NASS," *Int. J. Theor. Phys.*, vol. 57, no. 12, pp. 3745–3760, 2018.

XIANHUA SONG received the B.S. and M.S. degrees in computational mathematics from Jilin University, in 2005 and 2007, respectively, and the Ph.D. degree in computer science and technology from the Harbin Institute of Technology (HIT). She is currently an Associate Professor with the School of Science, Harbin University of Science and Technology, China. Her research interests include quantum computation, multimedia security, and machine learning.

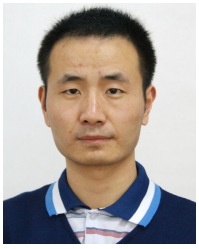

GUANGLONG CHEN received the M.S. degree in computational mathematics from the Harbin University of Science and Technology, in 2022. He is currently pursuing the Ph.D. degree in computational mathematics with Lanzhou University, focusing on solving partial differential equation inverse problems and medical imaging from machine learning perspective. His research interests include information security and quantum computation.

AHMED A. ABD EL-LATIF (Senior Member, IEEE) received the B.Sc. degree (Hons.) in mathematics and computer science and the M.Sc. degree in computer science from Menoufia University, Egypt, in 2005 and 2010, respectively, and the Ph.D. degree in computer science and technology from the Harbin Institute of Technology (HIT), Harbin, China, in 2013. He is currently an Associate Professor of computer science with Menoufia University, and the EIAS Data Science Laboratory, College of Computer and Information Sciences, Prince Sultan University, Saudi Arabia. He is the author and the coauthor of more than 200 articles, including refereed IEEE/ACM/Springer/Elsevier journals, conference papers, books, and book chapters. He has currently many books, more than ten books, in several publishers in Springer, IET, CRC Press, IGI-Global, Wiley, and IEEE. His research interests include multimedia content encryption, secure wireless communication, the IoT, applied cryptanalysis, perceptual cryptography, secret media sharing, information hiding, biometrics, forensic analysis in digital images, and quantum information processing. He is a fellow at the Academy of Scientific Research and Technology, Egypt, and a member of ACM. He received many awards, the State Encouragement Award in Engineering Sciences 2016, Arab Republic of Egypt; the Best Ph.D. Student Award from the Harbin Institute of Technology, China, in 2013; and the Young Scientific Award, Menoufia University, in 2014. He is the chair/co-chair/program chair of some Scopus/ EI conferences. He is the EIC of International Journal of Information Security and Privacy, and a Series Editor of the Advances in Cybersecurity Management (https://www.routledge.com). He is also an academic editor/associate editor for set of indexed journals (Scopus journals' quartile ranking).

MUDASIR AHMAD WANI received the M.C.A. and M.Phil. degrees in data mining from the University of Kashmir (UoK), in 2012 and 2014, respectively, and the Ph.D. degree in computer science from Jamia Millia Islamia (A Central University), New Delhi, India, in 2019. He was a Postdoctoral Researcher with the Norwegian Biometrics Laboratory, Norwegian University of Science and Technology (NTNU), Norway. He is currently working as a Lecturer and a Researcher with the Department of Information Security and Communication Technology (IIK), NTNU. He is actively involved in organizing and reviewing international conferences, workshops, and journals. His research interests include extraction and analysis of social data, and application of different statistical and machine/deep learning techniques in developing prediction models.

BASSEM ABD-EL-ATTY received the B.S. degree in physics and computer science, and the M.Sc. and Ph.D. degrees in computer science from Menoufia University, Egypt, in 2010, 2017, and 2020, respectively. He is currently an Assistant Professor with the Faculty of Computers and Information, Luxor University, Egypt. He is the author and coauthor of more than 40 papers, including refereed IEEE/Springer/Elsevier journals, conference papers, and book chapters. He is a reviewer in a set of reputable journals in Elsevier and Springer. His research interests include quantum information processing and image processing.